PRAMANA
— journal of
physics

Vol. 59, No. 4
October 2002
pp. 563–573

Hiss emissions during quiet and disturbed periods

D K SINGH[1] and R P SINGH[2]
[1]Indian Institute of Tropical Meteorology, Pune 411 008, India
[2]Department of Physics, Banaras Hindu University, Varanasi 221 005, India
Email: dksingh@tropmet.res.in; anshidevendra@rediffmail.com; rampal@banaras.ernet.in

MS received 17 July 2001; revised 11 March 2002

Abstract. The characteristic features of VLF hiss emissions during quiet and disturbed conditions observed at ground stations and on-board satellites are summarized. The increased intensity of the hiss emissions during magnetic storm period is explained by considering the enhanced flux of energetic electrons during magnetic storm period. The generation and propagation mechanism of VLF hiss are also briefly discussed.

Keywords. Coherent/incoherent Cerenkov radiation; ELF/VLF hiss emission; ionosphere; magnetosphere; wave–particle interaction; whistler mode waves.

PACS Nos 94.20.Rr; 94.30.Tz; 94.30.Hn

1. Introduction

Hiss emission is similar to whistler wave generated during atmospheric lightning, as waves share the same frequency, polarization, wave normal angle distribution and propagation mode. The only difference lies in their spectral form, i.e., whistlers are dispersed waves whereas hiss emissions present a band limited thermal noise spectrum producing a hissing sound. VLF hiss activity observed at ground stations spread in latitude and longitude varies from station to station. Satellite observations indicate that broad band hiss is present almost continuously in plasmasphere [1,2]. Global distribution of hiss is characterized by three principal zone of intense activity of which the first zone is located around invariant latitudes above 70° (auroral hiss), the second near 50° (mid-latitude) and the third below 30° latitude (equatorial hiss) [3]. Ground-based observations revealed that the low-latitude hiss are less intense than those observed at middle and high latitudes [4,5]. Jorgensen [6] analyzed amplitude distribution of hiss and showed that it decreased with decreasing latitude (10 dB per 1000 km) and explained it in terms of attenuation of hiss emission propagating through the earth-ionosphere wave guide from auroral zone to middle and low latitudes. Thus, low and middle latitude hiss events were also considered to be a part of the auroral hiss emissions [7,8]. Salient features of mid-latitude/plasmaspheric hiss and auroral hiss have been reviewed by Hayakawa and Sazhin [9] and Sazhin *et al* [10] respectively. Hiss emissions are classified into two types: continuous hiss and impulsive hiss. Spectrum

structure of continuous hiss does not reveal any large change for several minutes and even for hours. On the other hand impulsive hiss spectra can change considerably, even within seconds [11]. Impulsive hiss were mostly observed at mid- and high-latitude ground stations. Recently, impulsive hiss were observed at low latitude station Varanasi. Savchenko and Vaisman [12] have reported VLF hiss bursts associated with whistlers. On the basis of an analysis of experimental measurement and numerical simulation, they have shown that the VLF bursts observed on the ground can be formed by refraction and scattering of the VLF waves in the ionosphere on irregularities generated during the precipitation of energetic electrons induced by whistlers.

The intensity and dynamic spectrum of VLF hiss can be explained by analyzing two aspects of the problem; the principal mechanism of hiss generation and the propagation of hiss in the magnetosphere and the ionosphere. Both these processes are involved in the formation of dynamic spectra. However, their separate consideration sometimes results in considerable simplification of the problem, which is necessary for a better understanding of the physical background of the process. A number of generation mechanism both incoherent (Cerenkov radiation, cyclotron radiation, Doppler-shifted cyclotron radiation) and coherent (Cerenkov instability, cyclotron instability, traveling wave-tube mechanism) have been proposed from time to time to explain the observed hiss emission intensity at ground stations as well as on-board rockets and satellites [13–22]. In all the theoretical treatments of instability mechanism it was assumed that all the waves are amplified around the magnetic equator while propagating back and forth along the geomagnetic field lines, till their intensity reaches the observed intensity [4,23–28]. In the case of incoherent generation mechanism, the wave amplitude, generated by individual charged particle distributed along the field lines, is added up to explain the observed flux density. Solomon *et al* [29] have shown experimentally that amplification of background noise to the level of observed hiss intensity is possible. Based on DE-1 satellite data, Sonwalkar and Inan [30] proposed that the wave energy introduced in the magnetosphere by atmospheric lightning discharge may play an important role in embryonic generation of hiss emission.

2. Experimental data

Hiss emissions are characterized by spectral structure and polarization of the waves. Polarization measurement facilitates the identification of the mode of propagation and their arrival direction [31]. Ground-based impulsive auroral hiss shows circular polarization [32] indicating that it had penetrated through the ionosphere above the station and corresponded to parallel-propagating whistler-mode wave [33]. The polarization of continuous hiss is random [10]. Auroral hiss with right-hand elliptical polarization were also observed [34] indicating non-parallel wave propagation. Hayakawa *et al* [35] have reported right-handed circular polarization for the ELF hiss in the frequency range 1–2 kHz observed at Moshiri station. All these observations suggest hiss emissions to propagate in the whistler mode because no other mode with such a polarization can exist in this frequency range in the magnetospheric and the ionospheric plasma.

Hiss spectrum is similar to band-limited thermal noise in a wide frequency range up to several hundred kilohertz (only for the impulsive hiss). Continuous hiss dominates in the frequency range of 1–20 kHz [36]. The frequency range decreases as the location of station shifts towards low latitudes. The average power flux spectral density observed at

auroral zone stations was $\sim 10^{-16}$ W m^{-2} Hz^{-1} [6] with peak value greater than 10^{-14} W m^{-2} Hz^{-1} around 10 kHz. OGO-2 data revealed power flux spectral density two orders of magnitude higher than that on the ground [6]. Hiss power flux spectral densities up to 2×10^{-11} W m^{-2} Hz^{-1} had been reported on the basis of Injun-5 data [37] and Alouette-2 data [38]. Gurnett and Frank [37] had also reported an association between hiss bands and intense electron fluxes. They had also found the VLF hiss to be propagating generally downwards along the geomagnetic field lines. The data obtained on-board many satellites such as OGO-4 [39], Injun-5 [40], OGO-6 [41] ISIS-1 [42], S3-3 [43] and AUREOL/ARCAD3 [44] showed that auroral hiss emissions were well correlated with the electron fluxes at energies less than 1 keV. Further, when the electron fluxes decreased down to the level 10^4–10^5 electrons cm^{-2} s^{-1} ster^{-1} eV^{-1}, the auroral hiss power flux abruptly decreased below the recording level of Injun-5 [37]. Some times, hiss emissions have V-shaped spectrograms which are called as V-shaped hiss [37,45–47] or funnel-type hiss emissions [48]. Poynting vector for V-shaped hiss is downward along the field lines whereas V-shaped saucer emissions have upward wave normal direction [46]. Recently, Lalmani *et al* [49] reported VLF saucer emissions from the low latitude ground station Jammu.

The early observations of low latitude ground-based VLF hiss comes from Japanese workers [50–52] and later on from Indian workers [4,53]. VLF hiss at Srinagar, India was recorded in the frequency band 1–3 kHz and 5–7 kHz [53]. Singh *et al* [4] have reported VLF hiss observed at Varanasi in the frequency band 0.4–2.6 kHz and 4.6–6.1 kHz. They have also reported that the relative intensities of hiss events vary with frequency and time in the same event and also vary widely from event to event. Some of the events presented by Singh *et al* [4] belonged to mid-latitude hiss which had reached the ground station Varanasi, following the earth-ionosphere waveguide path after exiting from the mid-latitude magnetospheric ducts. Mid-latitude hiss has narrow band around 5 kHz, which is a typical property of mid-latitude storm-time hiss.

3. VLF hiss and magnetospheric disturbances

Simultaneous measurements of VLF hiss and electron fluxes supported the idea that hiss events are generated from electron fluxes present in the magnetosphere and ionosphere. During magnetic disturbances more particles are injected and hence, the occurrence probability of VLF hiss is increased. Some studies have been reported using K_{p} and AE indices. Analyzing the Syowa station data, it had been shown that the occurrence probability of auroral hiss increased when the K_{p} index increased from 0 to 5 and decreased when K_{p} value increased further [54]. They have also reported similar K_{p} dependence of hiss intensity at different frequencies. Jorgensen [55] reported that hiss bursts were not distinctly correlated with magnetic activity (measured by AE index). Enhanced hiss activity were found to be delayed 1 or 2 days with respect to magnetic storm. Impulsive hiss were reported during the expansion phase of a substorm in the mid-night sector whereas continuous hiss did not show any correlation with the local magnetic disturbances [36,56].

Substorm-associated mid-latitude VLF/ELF emissions could be easily associated with the injection of plasma-sheet electrons into the inner magnetosphere. Hence, substorm aspects of ELF/VLF emissions make it possible to investigate the wave–particle interaction process, the injection and drift process of particle during substorm, the magnetospheric

plasma structure etc. [57,58]. VLF emissions are intensified during magnetic disturbances and they exhibit a regular frequency drift in the dawn sector [57,58]. The frequency drift could be interpreted in terms of combined effect of the velocity dispersion during the eastward longitudinal drift of energetic electrons injected near the mid-night sector and a quasi-linear electron cyclotron generation of VLF waves [59]. Tsurutani *et al* [60] examined the dependence of inner zone hiss on the level of geomagnetic activity using AE (to identify substorms) and Dst (to identify storms) indices. They have reported that 92% of the hiss events occurred during active intervals containing a substorm (AE $> 100\gamma$), a magnetic storm or in most cases both. Fifty five percent of the events occurred during intense magnetic storms with peak $|\mathrm{Dst}| > 45\gamma$. Most of the storm time events occurred during the recovery phase as had been earlier reported by Smith *et al* [61]. Further, the most intense emissions occurred soon after the onset of a storm recovery phase. During low geomagnetic activity period hiss intensity was 10^2 orders of magnitude lower than the average intensity during the disturbance period. Analyzing Moshiri data, Hayakawa *et al* [35] showed that the occurrence rate of ELF hiss abruptly increases when $K_\mathrm{P} > 4$. There is a broad maximum in the occurrence rate for the K_P range from 5 to 7. Assuming that ELF hiss are caused by the trapped electron fluxes, it is interesting to see its variation with K_P values. Etcheto *et al* [62] had shown that the trapped flux does not vary significantly for values of K_P smaller than 2–3. Trapped flux increases rapidly for $K_\mathrm{P} > 3$–4. The measured flux as a function of K_P [36] fitted with that theoretically derived by Etcheto *et al* [62].

VLF hiss observed at low latitudes could trace their source region located at mid-latitude and at the equatorial zone [4,9]. Ariel satellites have provided a lot of evidence supporting the association of equatorial VLF hiss with thunderstorm activity [52]. Hayakawa *et al* [50] reported two types of VLF hiss recorded at low latitude stations: one was the storm-time VLF hiss centered around 5 kHz and the other was the quiet-time hiss. The former storm-time hiss were mid-latitude hiss generated around the plasma pause and they were observed at low latitudes after penetration at mid-latitudes, followed by the earth-ionosphere wave guide propagation. Quiet-time hiss were peculiar to lower latitudes. Hayakawa [52] had suggested that the hiss events reported by Khosa *et al* [53] could be storm-time plasmaspheric/mid-latitude hiss. It seems that some of the hiss events recorded at Varanasi in the frequency range 4–6 kHz could belong to storm-time mid-latitude VLF hiss.

4. Generation mechanism

The generation mechanism along with propagation mode should be able to explain the observed frequency spectrum, polarization and intensity of VLF hiss. The observed close correlation between auroral hiss and precipitating low energy electron fluxes made it possible to consider the latter as an energy source. The earliest suggested mechanism for the energy transfer from the electron to the wave was incoherent Cerenkov radiation [63]. It can occur regardless of plasma stability conditions and the emitted wave is broad band, covering the observed frequency range. For different regions of the ionosphere and magnetosphere, the power radiated from different models of the energetic electrons had been computed [4–6,8,18,40,64–66] and the results were compared with the observed power for mid and high latitudes. For ready reference we present selected results in figure 1. In the figure, average representative value of Injun-5 and Alouette-2 measurements are also shown. The measured spectral density in the frequency range from 1 kHz to 25 kHz lies

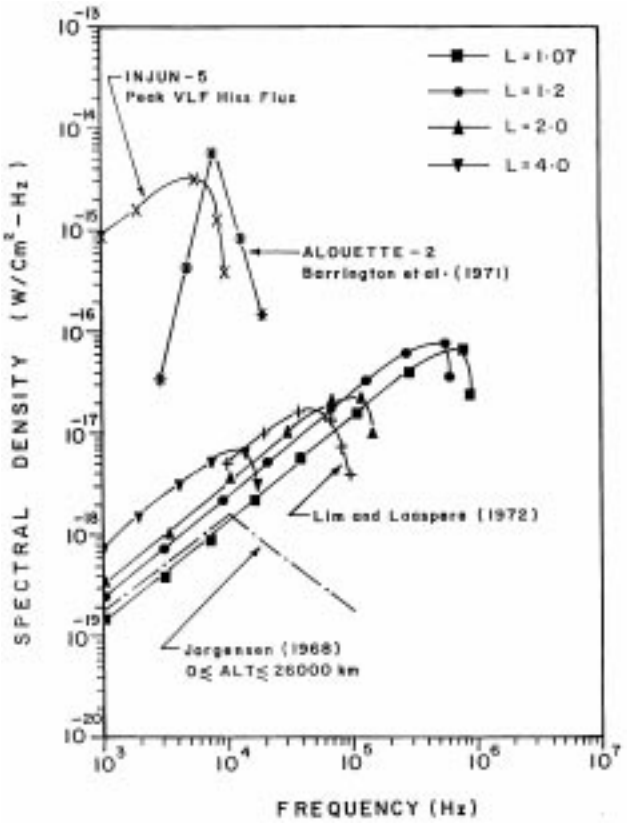

Figure 1. Observed spectral density (Injun-5, Alouette-2) and computed spectral density (from different models) in the frequency range 1 kHz–1 MHz.

between 10^{-16} and 10^{-14} W cm^{-2} Hz^{-1}. In the same frequency range, the computed power lies in the range $10^{-18} - 2 \times 10^{-17}$ W cm^{-2} Hz^{-1}. Thus, the computed spectral density falls short of observed power. In the computation of total power it has been assumed that all the electrons radiate in phase and emitted waves are guided along the field lines. From the figure it is also noted that the wave up to 1 MHz can be emitted through the Cerenkov process and the emitted power at higher frequencies are larger as compared to the power at lower frequencies. The waves while propagating towards the earth's surface are attenuated. Higher frequencies will have larger attenuation as compared to lower frequencies. In fact, the attenuation is minimum around 5 kHz and increases as frequency is either increased or decreased. If we take into account attenuation of the wave, non-guided wave propagation and random phase of the emitted waves, then the theoretically estimated power will be decreased and the gap between the measured and computed spectral densities will be increased.

From figure 1, it is also noted that the shape of the computed spectrum by Jorgensen [6] was similar to that of the Injun-5 data. Both have peak around 10 kHz. Similar spectrum has been reported by Singh *et al* [4] from slightly different radiating zone, that is $L = 4$.

Computations using improved model showed that the peak intensity corresponded to 70 kHz [18]. The reported results were more closer to the data obtained from Alouette-2 [38]. Theoretically computed power from lower L values show that as L value decreases, the frequency corresponding to maximum power increases. Also, the radiated power increases. It is clearly seen from figure 1. In the absence of power measurements at higher frequencies

Table 1. Measured and computed hiss intensity.

Frequency	Measured/Computed power	Reference
1–5 kHz	Measured power on-board satellite Injun-5 is 1.5×10^{-11} W m^{-2} Hz^{-1}	[67]
	Measured power on ground station is $\sim 10^{-14}$ W m^{-2} Hz^{-1}	[11]
	Observed power on the ground station, Moshiri (geomg. lat. 34° 5′N), is 5.4×10^{-18} W m^{-2} Hz^{-1}.	[68]
	Calculated power ($E >$10 eV) for $L = 1.07$ and 1.2 is 10^{-15} W m^{-2} Hz^{-1}	[69]
	Observed power on the ground station, Haraiso (geomag. lat. 26.7°N) is 4.4×10^{-19} W m^{-2} Hz^{-1}	[70]
	Calculated power (from the equatorial region) at $L = 4$, 2, 1.2, and 1.07 is $\sim 4 \times 10^{-25}$, 7×10^{-24}, 9×10^{-24}, and 5×10^{-24} W m^{-3} Hz^{-1} respectively	[4]
	Calculated power at the earth surface along $L = 4$ is $\sim 10^{-15}$ W m^{-2} Hz^{-1}	[4]
	Calculated power at the earth surface along $L = 2$, 1.2, and 1.07 is $\sim 10^{-15}$ to 10^{-14} W m^{-2} Hz^{-1}	[4]
6–10 kHz	Measured power on-board satellite Injun-3 is 10^{-12} W m^{-2} Hz^{-1}.	[67]
	Measured power on-board satellite Aloutte-2 is 2×10^{-12} W m^{-2} Hz^{-1}	[38]
	Computed power from electrons in a flux tube having length $0 \leq$ ALT $\leq 26,000$ km is 2.6×10^{-13} W m^{-2} Hz^{-1}	[6]
	Observed power at ground station Nord (geomag. lat. 80.8°N) is 10^{-14} W m^{-2} Hz^{-1}	[7]
	Observed power at ground station Macquarie Island (geomag. lat. 61.1°S) is 6.5×10^{-14} W m^{-2} Hz^{-1}	[71]
	Calculated peak intensity at 10 kHz is 3.5×10^{-13} W m^{-2} Hz^{-1}	[65]
	Measured power on-board satellite OGO-2 is 10^{-11} W m^{-2} Hz^{-1}	[6]
11–100 kHz	Total power intensity computed from the whole radiating region is 1.2×10^{-11} W m^{-2} Hz^{-1} at 70 kHz	[18]
	Calculated peak power intensity for $L = 4$ from the equatorial region is $\sim 10^{-24}$ W m^{-3} Hz^{-1} and at the earth surface is $\sim 6.78 \times 10^{-14}$ W m^{-2} Hz^{-1}	[4]
	Calculated peak power intensity at $L = 2$ from the equatorial region is $\sim 4 \times 10^{-22}$ W m^{-3} Hz^{-1} and at the earth surface is $\sim 2.3 \times 10^{-14}$ W m^{-2} Hz^{-1}	[4]
101–1000 kHz	Calculated peak power intensity from the equatorial region is $\sim 2 \times 10^{-21}$ W m^{-3} Hz^{-1} and at the earth surface $\sim 7.64 \times 10^{-13}$ W m^{-2} Hz^{-1}, for $L = 1.2$	[4]
	Calculated peak power intensity from the equatorial region is $\sim 5 \times 10^{-21}$ W m^{-3} Hz^{-1} and at the earth surface is $\sim 6.6 \times 10^{-13}$ W m^{-2} Hz^{-1} for $L = 1.07$	[4]

and low latitudes, we cannot test the above theoretical results. However, Hayakawa [52] had summarized the essential features of equatorial VLF hiss for $L < 1.2$ and had reported flux density $\sim 10^{-14}$ W m^{-2} Hz^{-1} for the wave frequencies 5–10 kHz. Thus, if we neglect the attenuation of the emitted wave then the average observed peak density can be explained. For the purpose of comparison, in table 1, we have summarized the available measured and the theoretically computed spectral density of the hiss events.

To explain the reported peak intensities of the equatorial VLF hiss $\sim 10^{-12}$ W m^{-2} Hz^{-1}, Singh *et al* [4] considered amplification of the incoherently radiated waves. The wave growth can take place when wave phase velocity corresponds to the region where $\left.\frac{\partial F_0}{\partial v}\right|_{v=\omega/k} > 0$, where F_0 is the electron distribution function [20,27,33]. The analysis of this instability for the generation of VLF hiss using different models for the electrons was considered by many workers [4,20,42,62,72–74]. The computed linear growth rate usually comes out to be small and to explain the observed spectral power, the wave has to bounce back and forth along the field line many times [4,31,74]. The wave is amplified each time it passes through the equatorial region [4,74]. During multiple bouncing, the signal having different intensity may couple from one duct to another and produce structureless signals of constant intensity as is observed in the case of ELF/VLF hiss. Further, during wave–particle interaction amplitude of the wave develops exponentially with time and it becomes essential to compute the final amplitude of the wave including non-linear effects in the wave–particle interaction. One may consider quasi-linear theory of wave–particle interaction to explain the details of observed dynamic spectra. Trakhtengerts *et al* [75] have discussed that the step-like deformation of the distribution function at the boundary between resonant and non-resonant electron leads to the strong amplification (2 orders of magnitude greater than that for a smooth distribution function). The role of inhomogeneous magnetic field [76] should also be included in the final computation of hiss spectra.

If N particles radiated incoherently then the total radiated power $P_T = NP$, where P is the power radiated by each particle. If the particles are phase-bunched, then they radiate coherently and the total radiated power P_T would be N^2P [65]. Thus, even small number of electrons emitting coherently could substantially increase the estimated power level. It has been shown that the trapped flux of precipitated electrons increases from 10^2 m^{-3} s^{-1} to 10^4 m^{-3} s^{-1} for $L = 4$ as K_p value increases from 2–3 to > 6 [62,77]. This shows that the radiating electron flux increases by a factor of 10^2 during magnetic storm conditions. If all the electrons radiated coherently then the estimated power flux would increase by a factor of 10^4 and we can easily explain the measured large hiss intensity during magnetically disturbed conditions. The intensity of the trapped flux is 10^3 m^{-3} s^{-1} for $K_p \cong 4$–5. Thus, even for moderate storm the flux increases by a factor of 10 and hence incoherent power would increase by a factor of 10, whereas coherently radiated power would enhance by a factor of 10^2. In all cases, hiss intensity would increase during magnetic storm period, which had been observed both on the ground as well as on the satellites.

The generation mechanism of VLF hiss remains controversial despite extensive theoretical and experimental work because, both the Cerenkov radiation and the wave–particle interaction mechanism required wave propagation parallel to the geomagnetic field lines, although, experimental data show that hiss often propagates at oblique angles and may originate in source region with relatively high wave-normal angles [30]. Sonwalkar and Inan [25] have shown that a hiss-like signal often follows lightning-generated whistlers. Draganov *et al* [78] based on ray-tracing simulations and estimates of whistler wave damping suggested that lightning-generated whistler wave energy can develop into plasma-

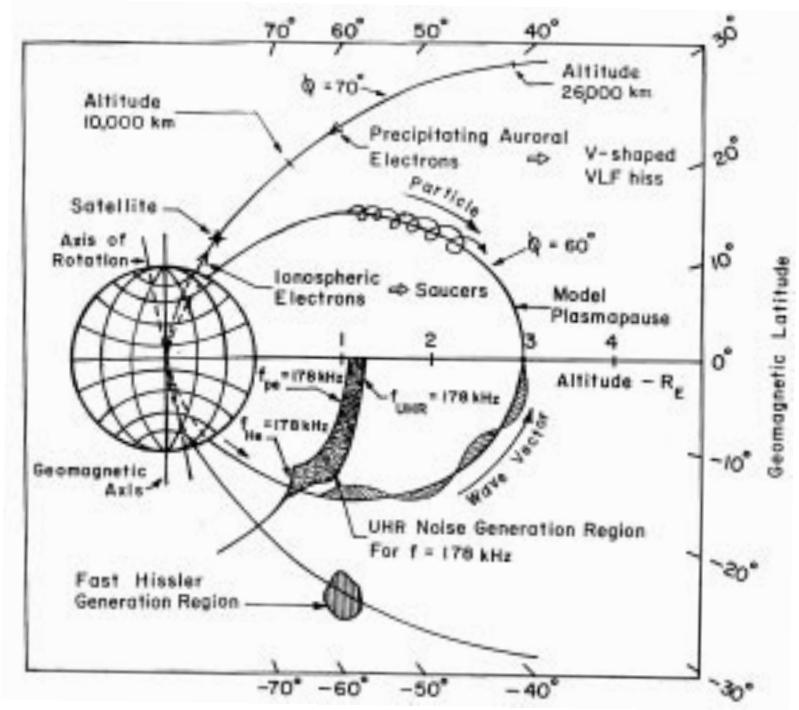

Figure 2. Generation region of the V-shaped hiss, upper hybrid resonance wave, saucers and fast hisslers. The figure is based on the model used for the computation of Cerenkov power to explain the above mentioned hiss emissions.

spheric hiss via multiple reflections, and thunderstorm activity on global scale may be sufficient to support observed hiss level. Recently, Savchenko and Vaisman [12] have presented VLF hiss preceding the whistlers. Based on the data analysis and numerical simulations they have shown that the VLF hiss bursts observed on the ground could have been formed by refraction and scattering of the VLF waves in the ionosphere on irregularities generated during the precipitation of energetic electrons induced by whistlers.

Apart from the continuous and periodic hiss, V-shaped hiss were also observed, which are characterized by the spectrum in which frequencies first decrease and then increase on a time scale from a few seconds to more than 30 s. They were observed while propagating downward along the field lines [30]. Cerenkov radiation mechanism had been proposed as the possible generation mechanism [37,45]. Similar to VLF hiss, band limited waves near upper hybrid resonance frequency had also been observed by rockets and satellites in the magnetosphere. The probable generation mechanism had been suggested to be Cerenkov radiation mechanism [18,79,80]. Siren [81] reported the observation of short duration auroral hiss burst showing an evidence of whistler mode dispersion in the frequency range 2–12 kHz with a maximum signal intensity $\sim 10^{-17}$ W cm^{-2} Hz^{-1} at 3 kHz. These signals were termed as fast hissler and they were supposed to be generated by the Cerenkov process [81]. The proposed generation region was considered at an altitude of 15,000 km and it was assumed that the waves with initial wave-normal angles lying in the range 0.2°–2.3° only could reach the ground. The source region of the V-shaped hiss, UHR noise and fast hissler are shown in figure 2. It may be noted that all these variations of hiss emissions are

recorded in the magnetosphere and their generation mechanism is still unresolved. Further work is required to explain the observed dynamic spectra, polarization and mode of propagation from the source to the receiving site.

5. Conclusion

In this paper we have reviewed reported characteristic properties of VLF hiss emissions observed at ground station as well as on-board satellites. Characteristic features of VLF hiss observed during magnetospheric disturbances are also discussed. The waves are proposed to be generated by the Cerenkov radiation mechanism as a first step and then they are subsequently amplified by the energetic electrons present in the magnetosphere [4]. It is suggested that during the magnetospheric disturbance period injected electron population increases by a factor of 10^2, which may explain the enhanced intensity of hiss emissions during disturbed conditions. In the end, some other emissions are also indicated which have been explained in terms of Cerenkov mechanism.

Acknowledgements

DKS is grateful to Dr A K Kamra for his encouragement and critical advice and RPS is grateful to DST for partly supporting the work under the project ESS75/042/99. The authors thank Shri V V Deodhar for his help in the preparation of diagrams. The authors are also grateful to the anonymous referee for his constructive and valuable suggestions.

References

[1] R M Thorne, A J Smith, R K Burton and R E Holzer, *J. Geophys. Res.* **78**, 1581 (1973)
[2] A J Smith, M A Frandsen, B T Tsurutani, R M Thorne and K W Chan, *J. Geophys. Res.* **79**, 2507 (1974)
[3] K Bullough, B Denby, W Gibbons, A R W Hughes, T R Kaiser and A R L Tetnall, *Proc. R. Soc. London* **A343**, 207 (1975)
[4] D K Singh, Ashok Kumar Singh, R P Patel, R P Singh and Abhai Kumar Singh, *Ann. Geophys.* **17**, 1260 (1999)
[5] D K Singh, R P Patel and R P Singh, *Indian J. Radio and Space Phys.* **30**, 24 (2001)
[6] T S Jorgensen, *J. Geophys. Res.* **73**, 1055 (1968)
[7] T S Jorgensen, *J. Geophys. Res.* **71**, 1367 (1966)
[8] Lalmani, M Rao, V V Somayajulu and B A P Tantry, *J. Geomag. Geoelec.* **24**, 261 (1972)
[9] M Hayakawa and S S Sazhin, *Planet. Space Sci.* **40**, 1325 (1992)
[10] S S Sazhin, K Bullough and M Hayakawa, *Planet. Space Sci.* **41**, 153 (1993)
[11] R A Helliwell, *Whistler and related ionospheric phenomena* (Stanford University Press, Stanford, USA, 1965)
[12] P P Savchenko and G M Vaisman, *Geomagn. Aeron.* **39**, 99 (1999)
[13] J F Mckenzie, *Philos. Trans. R. Soc. London, Ser.* **A225**, 585 (1963)
[14] J F Mckenzie, *Phys. Fluids* **10**, 2680 (1967)
[15] R N Singh and R P Singh, *Ann. Geophys.* **25**, 629 (1969)
[16] R P Singh and R N Singh, *Ann. Geophys.* **25**, 639 (1969)

[17] R P Singh, *Ann. Geophys.* **29**, 227 (1972)
[18] T L Lim and T Laaspere, *J. Geophys. Res.* **77**, 4145 (1972)
[19] M J Rycroft, *Radio Sci.* **7**, 811 (1972)
[20] R P Singh, *Planet. Space Sci.* **20**, 2073 (1972)
[21] T Ondoh, Y Nakamura, S Watanabe, K Aikyo and T Murakami, *Planet. Space Sci.* **31**, 411 (1983)
[22] S R Church and R M Thorne, *J. Geophys. Res.* **88**, 7941 (1983)
[23] R A Helliwell, D L Carpenter, U S Inan and J P Katsufrakis, *J. Geophys. Res.* **91**, 4381 (1986)
[24] S S Sazhin, *Planet. Space Sci.* **35**, 1267 (1987)
[25] V S Sonwalkar and U S Inan, *J. Geophys. Res.* **94**, 6989 (1989)
[26] A B Draganov, U S Inan, V S Sonwalkar and T F Bell, *J. Geophys. Res.* **93**, 11401 (1993)
[27] B T Tsurutani and G S Lakhina, *Rev. Geophys.* **35**, 491 (1997)
[28] N Cornilleau-Wehrlin, R Gendrin, F Lefeuvre, M Parrot, R Grard, D Jones, A Bahnsen, E Ungstrup and W Gibbons, *Space Sci. Rev.* **22**, 371 (1978)
[29] J Solomon, N Cornilleau-Wehrlin, A Corth and G Kremser, *J. Geophys. Res.* **93**, 1839 (1988)
[30] V S Sonwalkar and U S Inan, *J. Geophys. Res.* **93**, 7493 (1988)
[31] R A Helliwell, *Modern radio science* (1993) p. 189
[32] L Harang and K N Hauge, *J. Atmos. Terr. Phys.* **27**, 499 (1965)
[33] S S Sazhin, *Whistler mode waves in a hot plasma* (Cambridge University Press, Cambridge, 1992)
[34] M Nishine, Y Tanaka, A Iwai, T Kamada and T Hirasawa, *Mem. Natl. Inst. Polar Res.*, Tokyo, Special Issue No 26, p. 81 (1983)
[35] M Hayakawa, T Okada and Y Tanaka, *J. Geophys. Res.* **90**, 5153 (1985)
[36] K Makita, *Mem. Natl. Inst. Polar Res.*, Tokyo, Ser. A. Aeronomy, No. 16 (1979)
[37] D A Gurnett and L A Frank, *J. Geophys. Res.* **77**, 172 (1972)
[38] R E Barrington, T R Hartz and R W Harvey, *J. Geophys. Res.* **76**, 5278 (1971)
[39] T Laaspere and R A Hoffman, *J. Geophys. Res.* **81**, 524 (1976)
[40] S R Mosier and D A Gurnett, *J. Geophys. Res.* **77**, 1137 (1972)
[41] T Laaspere and W C Johnson, *J. Geophys. Res.* **78**, 2926 (1973)
[42] H G James, *J. Geophys. Res.* **78**, 4578 (1973)
[43] D J Gourney, S R Church and P F Mizera, *J. Geophys. Res.* **87**, 10479 (1982)
[44] C Beghin, J L Rauch and J M Bosqued, *J. Geophys. Res.* **94**, 1359 (1989)
[45] D A Gurnett, S R Mosier and R R Anderson, *J. Geophys. Res.* **76**, 3022 (1971)
[46] S R Mosier and D A Gurnett, *J. Geophys. Res.* **74**, 5675 (1969)
[47] H G James, *J. Geophys. Res.* **81**, 501 (1976)
[48] I Kimura, K Hashimoto, I Nagano, T Okada, M Yamamoto, T Yoshino, H Matsumoto, M Ejiri and K Hayashi, *J. Geomag. Geolect.* **42**, 459 (1990)
[49] Lalmani, M K Babu, R Kumar, R Singh and A K Gwal, *Ultra Sci.* **11**, 381 (1999)
[50] M Hayakawa, Y Tanaka and J Ohtsu, *J. Atmos. Terr. Phys.* **37**, 517 (1975)
[51] M Hayakawa and Y Tanaka, *Nature* (London) **270**, 703 (1977)
[52] M Hayakawa, *J. Atmos. Electr.* **13**, 65 (1993)
[53] P N Khosa, Lalmani, R R Rausaria and M M Ahmad, *Indian J. Radio Space Phys.* **10**, 209 (1981)
[54] M Hayakawa, Y Tanaka and J Ohtsu, *J. Geophys. Res.* **80**, 86 (1975)
[55] T S Jorgensen, Progress in ELF and VLF emission studies on high latitudes, in *The radiating atmosphere* edited by B M McCormac (Reidel Dordrect, 1979)
[56] K Makita and H Fukunishi, *Rep. Japan Antarctic Res. Expedition*, Vol. 46 (1973) p. 172
[57] D L Carpenter, J C Foster, T J Rosenberg and L J Lanzerotti, *J. Geophys. Res.* **80**, 4279 (1975)
[58] M Hayakawa , Y Tanaka, S S Sazhin, T Okada and K Kurita, *Planet. Space Sci.* **34**, 225 (1986)
[59] M Hayakawa, *Planet. Space Sci.* **37**, 269 (1989)

[60] B T Tsurutani , E J Smith and R M Thorne, *J. Geophys. Res.* **80**, 600 (1975)
[61] E J Smith, A M A Frandsen, B T Tsurutani, R M Thorne and K W Chan, *J. Geophys. Res.* **79**, 2507 (1974)
[62] J Etcheto, R Gendrin, J Solomon and A Roux, *J. Geophys. Res.* **78**, 8150 (1973)
[63] G R A Ellis, *J. Atmos. Terr. Phys.* **10**, 303 (1957)
[64] H G James, *J. Geophys. Res.* **78**, 4578 (1973)
[65] W W L Taylor and S D Shawhan, *J. Geophys. Res.* **79**, 105 (1974)
[66] R P Patel and R P Singh, *Pramana – J. Phys.* **56**, 605 (2001)
[67] D A Gurnett, *J. Geophys. Res.* **71**, 5599 (1966)
[68] A Iwai, J Ohtsu and Y Tanaka, *Proc. Res. Inst. Atmos. Nagoya Uni.* **11**, 29 (1964)
[69] Lalmani, V V Somayajulu and B A P Tantry, *Indian J. Pure Appl. Phys.* **8**, 564 (1970)
[70] T Ondoh and S Isozaki, *J. Radio Res. Lab.* **15**, 133 (1968)
[71] R L Dowden, *Nature* (London) **87**, 677 (1960)
[72] T Yamamoto, *Planet. Space Sci.* **27**, 273 (1979)
[73] J E Maggs and W Lotko, *J. Geophys. Res.* **86**, 3439 (1981)
[74] D K Singh, *Study of whistler waves and VLF emissions observed at Varanasi*, Ph.D. Thesis (Banaras Hindu University, India, 1999)
[75] V Y Trakhtengerts, M J Rycroft and A G Demekhov, *J. Geophys. Res.* **101**, 13293 (1996)
[76] Y Hobara, V Y Trakhtengerts, A G Demekhov and M Hayakawa, *J. Geophys. Res.* **103**, 20449 (1998)
[77] W N Hess, *The radiation belt and magnetosphere* (Blaisdell, Waltham Mass, 1968) p. 262
[78] A B Draganov, U S Inan, V S Sonwalkar and T F Bell, *Geophys. Res. Lett.* **19**, 233 (1992)
[79] S J Bauer and R G Stone, *Nature* (London) **218**, 1145 (1968)
[80] S R Mosier, M L Kaiser and L W Brown, *J. Geophys. Res.* **78**, 1673 (1973)
[81] J C Siren, *Nature* (London) **238**, 118 (1972)